View metadata, citation and similar papers at core.ac.uk

brought to you by CORE

provided by Springer - Publisher Connector

Published for SISSA by Springer

Received: *September 5, 2012*
Accepted: *November 22, 2012*
Published: *December 11, 2012*

Gamma lines without a continuum: thermal models for the Fermi-LAT 130 GeV Gamma line

Yang Bai[a,b] **and Jessie Shelton**[c]

[a] *SLAC National Accelerator Laboratory, 2575 Sand Hill Road, Menlo Park, CA 94025, U.S.A.*

[b] *Department of Physics, University of Wisconsin, Madison, WI 53706, U.S.A.*

[c] *Department of Physics, Sloane Laboratory, Yale University, New Haven, CT 06520, U.S.A.*

E-mail: yangbai@physics.wisc.edu, jshelton@physics.harvard.edu

Abstract: Recent claims of a line in the Fermi-LAT photon spectrum at 130 GeV are suggestive of dark matter annihilation in the galactic center and other dark matter-dominated regions. If the Fermi feature is indeed due to dark matter annihilation, the best-fit line cross-section, together with the lack of any corresponding excess in continuum photons, poses an interesting puzzle for models of thermal dark matter: the line cross-section is too large to be generated radiatively from open Standard Model annihilation modes, and too small to provide efficient dark matter annihilation in the early universe. We discuss two mechanisms to solve this puzzle and illustrate each with a simple reference model in which the dominant dark matter annihilation channel is photonic final states. The first mechanism we employ is resonant annihilation, which enhances the annihilation cross-section during freezeout and allows for a sufficiently large present-day annihilation cross section. Second, we consider cascade annihilation, with a hierarchy between p-wave and s-wave processes. Both mechanisms require mass near-degeneracies and predict states with masses closely related to the dark matter mass; resonant freezeout in addition requires new charged particles at the TeV scale.

Keywords: Beyond Standard Model, Cosmology of Theories beyond the SM

ArXiv ePrint: 1208.4100

JHEP12(2012)056

Open Access

doi:10.1007/JHEP12(2012)056

Contents

1 Introduction

The existence of dark matter (DM) is one of the strongest pieces of evidence for physics beyond the Standard Model. Searches in cosmic rays for evidence of DM annihilation or decays are a cornerstone of the experimental effort to detect DM. Monochromatic photon lines, though in most models a subdominant signal, provide a particularly clean astrophysical signal [1–5].

Several recent analyses have claimed evidence for a distinct spectral feature in the Fermi-Large Area Telescope (LAT) [6] photon spectrum at around 130 GeV [7–10], in regions near the galactic center. Evidence for this feature has also been reported in galactic clusters [11] and in non-associated sources [12], although the latter claim remains contentious [13–15]. While the statistics are limited, the morphology of the signal may favor an explanation as annihilating DM [11, 16, 17]. The presence of an additional photon line at approximately 111 GeV [10, 12] is highly suggestive, if also statistically limited, and would lend more credence to a particle physics explanation [18]. The Fermi collaboration's own search for photon lines uses slightly different search regions and methodology and sets an upper limit marginally in conflict with the claimed signal [19].

It remains to be established whether the excess is instrumental, astrophysical, or representative of an overly optimistic characterization of the systematic uncertainties in the galactic background [20, 21]. However, standard thermal WIMPs are not capable of explaining the Fermi signal, and it is of interest to work out the necessary structure in DM models which could give rise to the 130 GeV line.

Any dark matter model for the Fermi 130 GeV line must account for two interesting facts. First, there is no evidence for an excess in the continuum photon spectrum, which strongly constrains DM annihilation into the usual SM annihilation channels ($f\bar{f}$, W^+W^-, ZZ) [17, 22–24] or indeed into any charged final states. Since in most thermal models

JHEP12(2012)056

DM-photon couplings are generated radiatively from the DM couplings to charged final states [25, 26], the typical line cross section is generically related to the cross-section for annihilation into charged modes $X, X^\dagger$ by

$$\langle \sigma v \rangle_{\gamma\gamma} \sim \left(\frac{\alpha}{\pi}\right)^2 \langle \sigma v \rangle_{XX^\dagger} \,. \tag{1.1}$$

As the fragmentation and decay of the final states $X, X^\dagger$ give rise to a continuum photon spectrum $d\Phi_\gamma(E)/dA \propto n_{DM}^2 \langle \sigma v \rangle_{XX^\dagger} dN_\gamma/dE$, if annihilation to charged states is open, the expected line flux is smaller than the continuum flux by several orders of magnitude. Models for the Fermi 130 GeV line must therefore explain the absence of annihilation into charged (or hadronic) modes.

This brings us to the second interesting fact. The best fit cross-sections for the 130 GeV feature [7, 8] are more than an order of magnitude smaller than the expectation for (s-wave) thermal freezeout. If annihilation to SM or charged modes is absent or suppressed as the continuum limits suggest, reconciling this inefficient annihilation to photons with the WMAP relic density $\Omega_\chi h^2 = 0.1109 \pm 0.0056$ [27] requires either: (1) a nonthermal relic abundance [28, 29]; (2) non-photonic annihilation modes which are suppressed, possibly only post-freezeout, relative to the naive radiative scaling of eq. (1.1) [29, 30]; or (3) a mechanism to enhance the thermal annihilation cross-section to photonic final states in the early universe [31–33].

In the present work we will study two mechanisms which give enhanced DM annihilation to photons while also obtaining the correct thermal relic abundance, and build simple reference models for both. Our first example is resonant freezeout, where the presence of a resonance in the DM sector spectrum enhances the annihilation cross-section into photons during freezeout. Our second example introduces an intermediate annihilation mode, so that DM annihilation proceeds through a cascade decay of a non-photonic intermediate state, $\bar{\chi}\chi \to \phi\phi' \to 4\gamma$. In this example, the relation between the cross-section necessary for thermal freezeout and the present-day gamma line cross section is explained by the interplay of s-wave and p-wave contributions to the annihilation.

In section 2, we perform an effective operator analysis of DM-photon couplings and demonstrate the need for new particles at mass scales comparable to the DM mass. In section 3 we perform a detailed examination of resonant freezeout, and consider cascade decays in section 4. Section 5 contains our conclusions.

2 Effective operators for DM annihilation to photons

To demonstrate the need for multiple new states in thermal models for the Fermi 130 GeV line, we begin by writing effective operators to describe the interaction between DM and one or two photons. We assume an unbroken $\mathbb{Z}_2$ symmetry to explain the stability of the DM particle, and for simplicity work after electroweak symmetry breaking. We first consider the case when DM is a (Dirac) fermion. The leading operators coupling DM to photons are the electric and magnetic dipole operators, $\overline{\chi}\sigma_{\mu\nu}\chi F^{\mu\nu}$ and $\overline{\chi}\sigma_{\mu\nu}\chi \tilde{F}^{\mu\nu}$, appearing at dimension five [34, 35]. However, the dominant annihilation process mediated by these two

JHEP12(2012)056

operators is $\chi\chi \to f\bar{f}$ through a photon in the s-channel [30]. This problematic annihilation to $f\bar{f}$ can be suppressed in the present day if the Dirac fermion is split into two Majorana $\chi_{1,2}$, with a small mass gap $m_2 - m_1$ such that the depleted abundance of the heavier χ_2 post-freezeout shuts off the charged annihilation channel [29, 30, 36]; in this case, the DM is the Majorana χ_1 and the EFT containing only χ_1 is indeed insufficient to describe the freezeout.

At dimension seven, there are four operators which couple DM pairs to two photons, two CP-conserving operators

$$\frac{c_1}{4\,\Lambda^3}\overline{\chi}\chi F_{\mu\nu}F^{\mu\nu} \;+\; \frac{c_5}{4\,\Lambda^3}\overline{\chi}\gamma_5\chi F_{\mu\nu}\tilde{F}^{\mu\nu}\,, \tag{2.1}$$

and two CP-violating operators

$$\frac{\bar{c}_1}{4\,\Lambda^3}\overline{\chi}\chi F_{\mu\nu}\tilde{F}^{\mu\nu} \;+\; \frac{\bar{c}_5}{4\,\Lambda^3}\overline{\chi}\gamma_5\chi F_{\mu\nu}F^{\mu\nu}\,. \tag{2.2}$$

In addition there are operators with a single photon, such as $\overline{\chi}\chi F_{\mu\nu}Z^{\mu\nu}$, $\overline{\chi}\gamma_5\chi F_{\mu\nu}\tilde{Z}^{\mu\nu}$, and $\overline{\chi}\gamma_\mu\chi F^{\mu\nu}\partial_\nu h$. We will concentrate on the operators with two photons, but we will comment on other operators when we introduce a concrete UV model.

For scalar DM, the first DM-photon interactions appear at dimension 6,

$$\mathcal{O}_{sc,1} = |\phi|^2 F_{\mu\nu}F^{\mu\nu}, \qquad \mathcal{O}_{sc,2} = |\phi|^2 F_{\mu\nu}\widetilde{F}^{\mu\nu}. \tag{2.3}$$

For simplicity we have taken ϕ complex, but this is not strictly necessary.

For fermionic DM, the presence of independent operators which contribute in different leading partial waves to the DM annihilation cross-section show that it is easy to accommodate an apparent suppression in the DM annihilation cross-section. In an EFT consisting of the CP-conserving operators in eq. (2.1), the cross-section is

$$\sigma v = \frac{m_\chi^4}{16\pi\Lambda^6}\left[4\,c_5^2 + (2\,c_5^2 + c_1^2)\,v^2\right] + \mathcal{O}(v^4) \equiv s + p\,v^2 + \mathcal{O}(v^4). \tag{2.4}$$

For a mixed partial wave freezeout process, the dark matter relic abundance is approximately given by [37]

$$\Omega_\chi h^2 \approx \frac{1.07\times 10^9}{\mathrm{GeV}\,M_{pl}\,\sqrt{g^*}}\,\frac{x_F}{s + 3(p - s/4)/x_F}\,, \tag{2.5}$$

in terms of the freeze-out temperature

$$x_F = \ln\left[\frac{5}{4}\sqrt{\frac{45}{8}}\frac{g}{2\pi^3}\frac{M_{pl}\,m_\chi(s + 6\,p/x_F)}{\sqrt{g^*}\sqrt{x_F}}\right]. \tag{2.6}$$

In figure 1 we show in the left panel the region of s and p giving the correct relic density, and in the right panel translate that into the region of operator coefficients c_1/Λ^3 and c_5/Λ^3. From figure 1, we can see that to simultaneously accommodate the thermal relic abundance and the best-fit cross section for the Fermi-LAT 130 GeV line requires a large hierarchy between p- and s-wave scattering, $p/s \approx 65$, or $c_1/c_5 \approx 12$.

JHEP12(2012)056

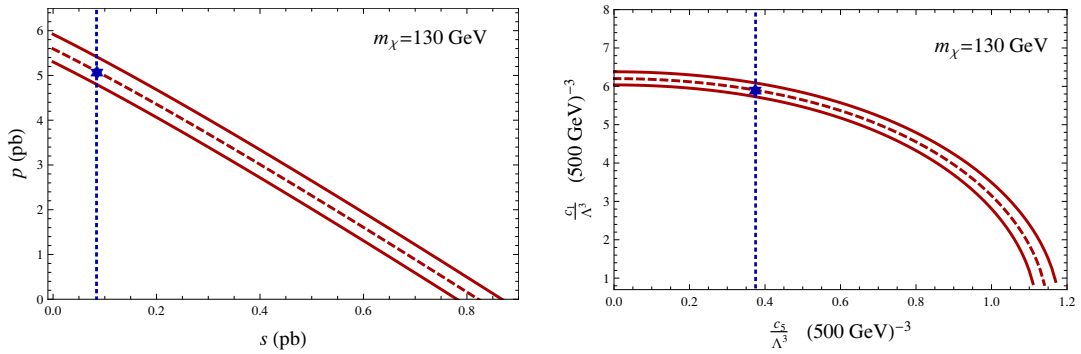

Figure 1. Left panel: the red solid lines are the allowed region of s and p cross sections in pb to satisfy the dark matter relic abundance within one σ. The blue dotted line denotes $s = 0.084$ pb·c, the present-day gamma line cross section in ref. [8] (Einasto profile). Our DM particle is a Dirac fermion, so the required cross section is a factor of two larger than the one for a Majorana fermion in ref. [8]. Right panel: same as the left, but in terms of operator coefficients c_1/Λ^3 and c_5/Λ^3. The effective number of relativistic degrees of freedom g_* is taken to be 75.75, $g_\chi = 4$, and $m_\chi = 130\,\text{GeV}$.

Figure 1 also shows that to obtain a reasonable relic abundance through annihilation to photons only, the cutoffs of the effective operators are order 500 GeV if c_1 and c_5 are order of unity. Unfortunately the natural magnitude of c_1 and c_5 is α/π, so without additional enhancement factors, the necessary cutoff Λ is much smaller than m_χ, invalidating the EFT.

In the next two sections, we study two models which extend some of the effective operators of in eq. (2.1) and eq. (2.2) by introducing a (pseudo-)scalar degree of freedom ϕ which couples to hypercharge gauge bosons through a loop of charged fermions,

$$\mathcal{L} = \frac{1}{2}\,\partial_\mu\phi\partial^\mu\phi + \bar{f}_i(i\partial\!\!\!/ - g_Y Y B\!\!\!/ - m_f)f_i - \lambda_\chi^r\bar{\chi}\chi\phi - \lambda_\chi^i i\bar{\chi}\gamma_5\chi\phi - y_f\phi\bar{f}_i f_i - \frac{m_\phi^2}{2}\phi^2\,, \quad (2.7)$$

where Y is the hypercharge of the new charged fermions f_i under $\mathrm{U}(1)_Y$, and $i = 1\cdots N_f$ is the flavor index of the N_f fermions. We integrate out f_i to generate the following effective operators [38]

$$\frac{N_f\, y_f\, Y^2\, \alpha_Y}{4\pi\, m_f}\,\frac{2}{3}\,\phi\, B_{\mu\nu}B^{\mu\nu} \supset \frac{N_f\, y_f \alpha\, e_f^2}{4\pi\, m_f}\,\frac{2}{3}\,\phi\, F_{\mu\nu}F^{\mu\nu} \equiv \frac{\alpha}{4\pi\,\hat{m}_f}\,\phi\, F_{\mu\nu}F^{\mu\nu}\,. \quad (2.8)$$

Here we have absorbed the electric charge e_f, the Yukawa coupling y_f and the multiplicity factor N_f into the definition of $\hat{m}_f$.[1] There are two more operators $F_{\mu\nu}Z^{\mu\nu}$ and $Z_{\mu\nu}Z^{\mu\nu}$ generated. We neglect these operators in our analysis, but we will also comment on how the analysis changes in the presence of additional final states which could be γZ and ZZ (see ref. [39] for using γZ as the dominant channel for the 130 GeV line). We also point out that if the $\sim 114\,\text{GeV}$ gamma line becomes robust, our analysis should be extended to include operators constructed from $W^a_{\mu\nu}$ to fit the relative fluxes in $\bar{\chi}\chi \to \gamma\gamma$ and $\bar{\chi}\chi \to \gamma Z$.

[1] If ϕ is a pseudo-scalar, coupling as $\phi\, i\,\bar{f}_i\gamma_5 f_i$, one needs to replace $\frac{2}{3} \times \phi B_{\mu\nu}B^{\mu\nu}$ by $1 \times \phi B_{\mu\nu}\tilde{B}^{\mu\nu}$.

JHEP12(2012)056

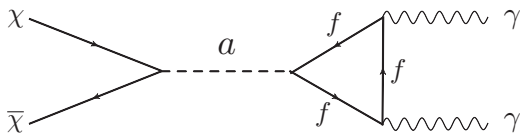

Figure 2. Feynman diagram for resonant annihilation.

3 Resonant freezeout

One way to enhance the dark matter annihilation cross section at freezeout relative to the cross-section today is by introducing a resonance with mass slightly above twice the DM mass,

$$m_a^2 = 4m_\chi^2(1+\delta)\,, \tag{3.1}$$

for $0 < \delta \ll 1$ [31, 40]. In this section we will discuss the parameter space for a resonant freezeout model where DM annihilation to photon pairs is entirely responsible for setting the thermal abundance. To be concrete, we consider a simple UV completion of the EFT in the previous section, namely Dirac fermionic dark matter χ coupling to photons through a pseudo-scalar a with

$$\mathcal{L} \supset -i\,\lambda_\chi^i \overline{\chi}\gamma_5\chi a - \frac{1}{4\Lambda} a\, F_{\mu\nu}\widetilde{F}^{\mu\nu}\,. \tag{3.2}$$

We take the loop-induced $aF\widetilde{F}$ coupling to be given by a loop of charged fermions, as shown in figure 2, so the effective coupling is

$$\frac{1}{\Lambda} = \frac{\alpha y_f N_f e_f^2}{\pi m_f} \equiv \frac{\alpha}{\pi \hat{m}_f}\,, \tag{3.3}$$

where y_f is the Yukawa coupling of a to the heavy fermions f whose mass, number, and charge are given by m_f, N_f, and e_f.

3.1 *s*-wave

The operators in eq. (3.2) yield the annihilation cross section

$$\begin{aligned}\sigma v &= \frac{m_\chi^4}{4\,\pi}\left(\frac{\alpha\lambda_\chi^i}{\pi\,\hat{m}_f}\right)^2 \frac{1}{\left[(4m_\chi^2 + m_\chi^2 v^2) - m_a^2\right]^2 + \Gamma_a^2 m_a^2} \\ &\equiv \frac{1}{64\,\pi}\left(\frac{\alpha\lambda_\chi^i}{\pi\,\hat{m}_f}\right)^2 \frac{1}{(\delta - v^2/4)^2 + \gamma^2(1+2\delta)}\end{aligned} \tag{3.4}$$

where Γ_a is the total width of a, $\gamma \equiv \Gamma_a/m_a$, and in the second line we have taken $v, \delta, \gamma \ll 1$ [31]. We can write the thermally averaged cross-section as

$$\langle\sigma v\rangle \equiv \langle\sigma v\rangle_\infty\, f(x;\delta,\gamma), \tag{3.5}$$

where $x \equiv m_\chi/T$,

$$\langle\sigma v\rangle_\infty = \frac{1}{64\pi}\left(\frac{\alpha\lambda_\chi^i}{\pi\hat{m}_f}\right)^2 \frac{1}{\delta^2 + \gamma^2(1+2\delta)} \tag{3.6}$$

JHEP12(2012)056

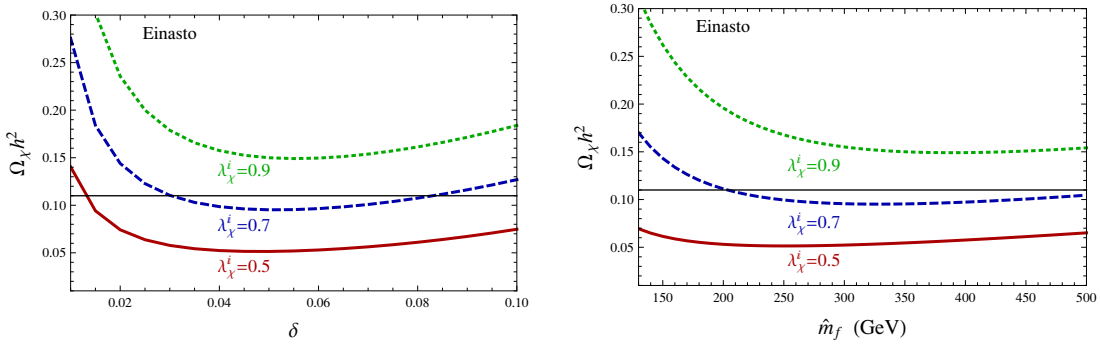

Figure 3. The dependence of the relic abundance $\Omega_\chi h^2$ on δ for different values of λ_χ^i (left) and $\hat{m}_f$ (right), with the present-day cross-section fixed to the (Einasto) best-fit value for the Fermi-LAT gamma line excess.

is the cross-section at $x \to \infty$, and

$$f(x;\delta,\gamma) = \frac{x^{3/2}}{\sqrt{4\pi}} \int v^2 dv\, e^{-xv^2/4} \frac{\delta^2 + \gamma^2(1+2\delta)}{(\delta + v^2/4)^2 + \gamma^2(1+2\delta)} \tag{3.7}$$

contains the information about the nontrivial velocity dependence of the cross-section. The width of the pseudo-scalar is bounded from below by its couplings to dark matter (in the relevant parameter space, the radiative width into photons is negligible). For $\delta \ll 1$,

$$\gamma = \frac{\sqrt{\delta}\lambda_\chi^{i\,2}}{8\pi}\left(1 - \frac{1}{2}\delta\right). \tag{3.8}$$

We first establish that our model has a reasonable range of parameter space which can give a sufficiently large cross-section for $\chi\bar{\chi} \to \gamma\gamma$. Requiring $\langle\sigma v\rangle_0 = \langle\sigma v\rangle_\infty f(x_0)$,

$$\left(\frac{64\pi^3 \hat{m}_f^2}{\alpha^2 \lambda_\chi^{i\,2}}\right)\langle\sigma v\rangle_0 = \left(\frac{\hat{m}_f/\lambda_\chi^i}{300\ \text{GeV}}\right)^2 \left(\frac{1}{0.06}\right)^2 = \frac{1}{\delta^2} f(x_0;\delta) \approx \frac{1}{\delta^2}\,, \tag{3.9}$$

where we have used the Einasto value for $\langle\sigma v\rangle_0$ and dropped terms of order γ^2. This determines $\hat{m}_f$ as a function of δ and λ_χ^i, showing that obtaining the present-day cross-section requires $\delta \lesssim 0.1$.

After using the present-day best fit cross-section to fix $\hat{m}_f$ in terms of λ_χ^i, δ, the thermal freezeout is controlled by δ and the minimum allowable width, as determined by eq. (3.8). Figure 3 illustrates the dependence of the final relic abundance on δ and λ_χ^i. Since the resonance sees significant overlap with the bulk of the velocity distribution during freezeout, the strength of the resonant enhancement to the cross-section is enhanced when γ is smaller, increasing the value of the cross-section at the pole. Therefore if γ is too small, e.g. $\lambda_\chi^i \leq 0.5$ in figure 3, the annihilation is too efficient and the yield is too small to account for the present-day dark matter abundance in the absence of other decay modes for a. If, on the other hand, γ is too large, e.g. $\lambda_\chi^i \geq 0.7$ in figure 3, annihilation is inefficient and could even over-close the universe. Annihilation becomes less efficient both gradually at large δ and rapidly at very small δ, as the pole passes outside the main peak of the Maxwell-Boltzmann distribution during freezeout.

JHEP12(2012)056

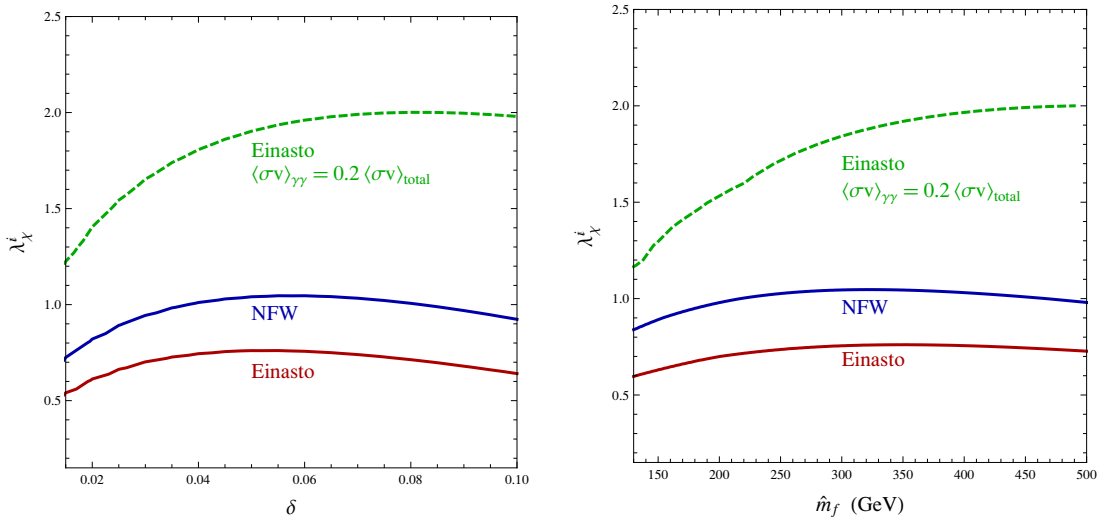

Figure 4. Contours in the δ-λ_χ^i plane (left) and $\hat{m}_f$-λ_χ^i plane (right) yielding $\Omega_\chi h^2 = 0.111$ for the s-wave resonance model after fixing present-day cross-sections to best-fit Fermi-LAT gamma line values. The dashed line is the contour for the present-day Einasto gamma line cross section with the assumption that $\mathrm{Br}(a \to \gamma\gamma) = 20\%$.

In figure 4 we show the contours in the δ-λ_χ^i plane yielding $\Omega_\chi h^2 = 0.11$. To illustrate the astrophysical uncertainties, we quote results for both the Einasto and NFW gamma line best-fit cross sections. Comparing the resulting contours, we can see that the astrophysical uncertainty introduces an order 50% uncertainty on the couplings of the pseudo-scalar to dark matter. In the green dashed line of figure 4, we show the contour for the case where a has an additional decay mode $XX^\dagger$ with $\mathrm{Br}(a \to XX^\dagger) = 5\,\mathrm{Br}(a \to \gamma\gamma)$.

As can be seen from figure 4, there is no real upper bound on the (scaled) fermion mass $\hat{m}_f$. However, from eq. (3.9), $\hat{m}_f$ is inversely proportional to δ, to obtain the present-day annihilation cross section. If one requires $\delta > 0.01$ from considerations of fine-tuning, the scale for the charged fermion masses should be bounded from above by around 500 GeV, or in other words, within collider-accessible energies.

3.2 $s + p$-wave

We now consider the case where more than one partial wave is important for freezeout. For concreteness we extend the single pseudo-scalar model of the previous subsection to include a CP-violating coupling $\lambda_\chi^r a\bar{\chi}\chi$ to the dark matter,

$$\mathcal{L} \supset -i\lambda_\chi^i \overline{\chi}\gamma_5\chi a - \lambda_\chi^r a\bar{\chi}\chi - \frac{\alpha}{4\pi\hat{m}_f} a\, F_{\mu\nu}\widetilde{F}^{\mu\nu}. \tag{3.10}$$

Pure p-wave freezeout would require extremely tuned values of the resonance mass, $\delta \sim 10^{-5}$, to obtain the present-day observed cross-section. In the more interesting case of mixed s and p-wave resonant freezeout, the present-day observed cross-section, and hence the necessary values of δ, are set by the s-wave contribution, but p-wave scattering can dominate the annihilation at freezeout. When p-wave scattering dominates freezeout, the

JHEP12(2012)056

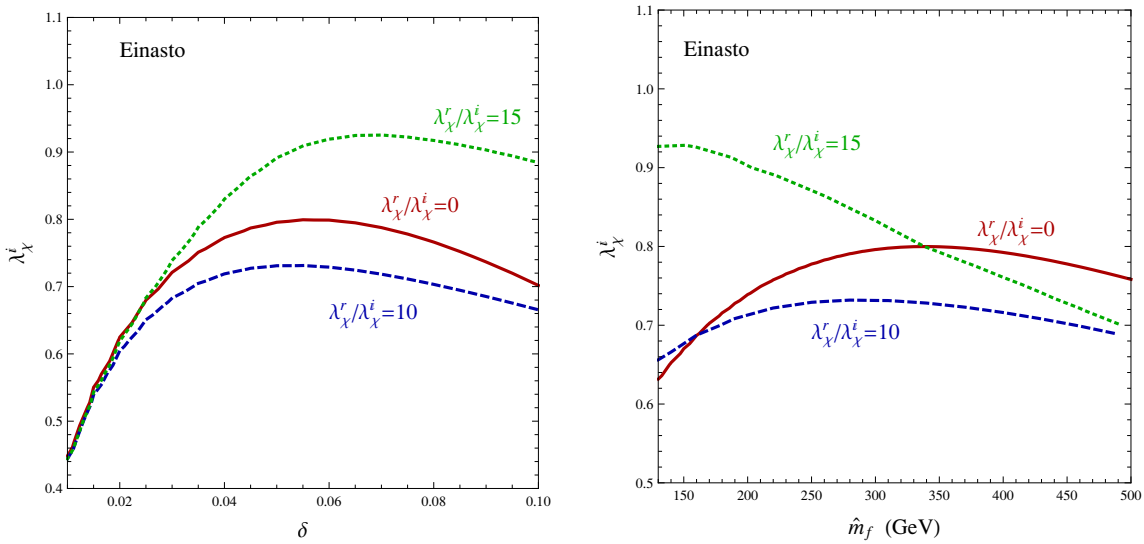

Figure 5. Contours in the δ-λ_χ^i plane (left) and $\hat{m}_f$-λ_χ^i plane (right) yielding $\Omega_\chi h^2 = 0.11$ in the $s+p$-wave resonance model, for different ratios of $\lambda_\chi^r/\lambda_\chi^i$ after fixing present-day cross-sections to best-fit Fermi-LAT gamma line values. Results are shown for the Einasto best fit cross-section for the gamma line excess.

additional v^2 dependence of the cross-section shifts the velocity integral to higher values, reducing the overlap with the pole; narrower resonances are therefore required to achieve cross-sections sufficiently efficient to yield the observed relic abundance. Therefore when p-wave scattering dominates during freezeout, additional contributions to the a width are more constrained than in the s-wave case. Since we will be interested in cases with a hierarchy between p-wave and s-wave modes, it is important to include the contribution to γ from λ_χ^r, $\gamma_r = \delta^{3/2}{\lambda_\chi^r}^2(1-\frac{1}{2}\delta)/(8\pi)$.

As for the pure s-wave case, we show the contours of $\Omega_\chi h^2 = 0.11$ in the δ-λ_χ^i and $\hat{m}_f$-λ_χ^i planes in figure 5. We plot three different ratios of $\lambda_\chi^r/\lambda_\chi^i$. For $\lambda_\chi^i \gtrsim \lambda_\chi^r\sqrt{\delta}$, the contribution to the resonance width from λ_χ^r is negligible. The additional p-wave contribution to the freeze-out cross section prefers a smaller value of λ_χ^i, which explains why the pure s-wave contour (red, solid) in the left panel lies at larger values of λ_χ^i than the blue dashed contour, which denotes a case where p-wave scattering is important for annihilation but not for the resonant width. For $\lambda_\chi^i \lesssim \lambda_\chi^r\sqrt{\delta}$, the contribution to the resonance width from λ_χ^r is non-negligible, reducing the enhancement from the resonance. As a result, larger values of λ_χ^i are required to obtain sufficiently efficient annihilation, as can be seen from the green, dotted contour in the left panel.

As can been from the right panel of figure 5, the photon vertex scale $\hat{m}_f$ is again below around 500 GeV for $\delta \gtrsim 0.01$, implying collider-accessible charged particles.

The new SM singlet scalar particles a may also couple to other SM fermions other than photon. Since only higher-dimensional operators can be written down for a to couple to fermions, we assume that the cutoffs of those operators are much higher than $\hat{m}_f$ and their effects on other physics like flavor physics and DM direct detection can be neglected.

JHEP12(2012)056

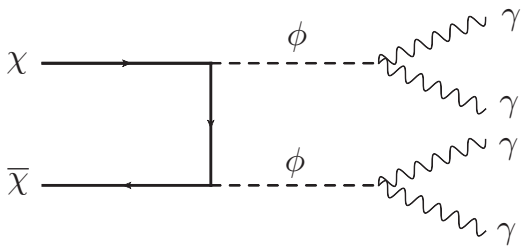

Figure 6. The Feynman diagram to describe DM cascade annihilation into four photons.

4 Cascade annihilation

Another way to reconcile the large photon line cross-section with the lack of continuum photons while obtaining the proper relic density is to have the dark matter first annihilate into (neutral) intermediate states, which then decay into photons. The advantage of extending the DM annihilation process with a cascade decay is that the relic abundance is now only controlled by the couplings of dark matter to the intermediate particles. The small radiative couplings of photons to the intermediate state are only relevant for the lifetime of that state, and are irrelevant for the annihilation cross section. The gamma ray signals from cascading DM annihilations have been discussed in [41–43] and applied to the Fermi-LAT gamma line excess in [9, 44]. Here, we write down a simple explicit model and discuss the parameter space for realizing a thermal relic abundance together with an explanation for the Fermi-LAT gamma line excess.

As before, we consider Dirac dark matter χ, together with a real scalar field which we denote ϕ, and study the following set of interactions

$$\mathcal{L} \supset -\lambda_\chi^r \overline{\chi}\chi\phi - i\lambda_\chi^i \overline{\chi}\gamma_5\chi\phi - \frac{\alpha}{4\pi\,\hat{m}_f}\phi\, F_{\mu\nu}F^{\mu\nu}\,. \tag{4.1}$$

Here, as before, the scale $\hat{m}_f \equiv 2N_f y_f e_f^2/3m_f$ arises from some heavy charged fermions that are integrated out to generate the ϕFF operator; we require only that m_f is sufficiently large to forbid DM from annihilating into charged fermions. We are interested in the parameter space where $m_\phi < m_\chi$, so the dominant annihilation channel for DM is $\overline{\chi}\chi \to \phi\phi \to 4\gamma$, as shown in figure 6.

The energies of the two photons from each ϕ decay are, in the dark matter rest frame,

$$E_{\gamma_{1,2}} = \frac{m_\chi}{2}\left(1 \pm \sqrt{1-\frac{m_\phi^2}{m_\chi^2}}\cos\theta\right)\,, \tag{4.2}$$

where θ is the angle between the photon direction in the ϕ rest frame and the ϕ direction of motion. Because ϕ is a scalar field, the distribution is isotropic in θ, and the photon spectrum is evenly distributed between the kinematic endpoints:

$$\begin{aligned}\frac{dN_\gamma}{N_\gamma dE_\gamma} &= \frac{1}{\sqrt{m_\chi^2-m_\phi^2}}\Theta\left[E-\frac{m_\chi}{2}\left(1-\sqrt{1-\frac{m_\phi^2}{m_\chi^2}}\right)\right]\Theta\left[\frac{m_\chi}{2}\left(1+\sqrt{1-\frac{m_\phi^2}{m_\chi^2}}\right)-E\right]\,,\\ &\xrightarrow{\epsilon\ll 1} \frac{1}{m_\chi\sqrt{2\epsilon}}\Theta\left[E-\frac{m_\chi}{2}\left(1-\sqrt{2\epsilon}\right)\right]\Theta\left[\frac{m_\chi}{2}\left(1+\sqrt{2\epsilon}\right)-E\right]\,,\end{aligned} \tag{4.3}$$

JHEP12(2012)056

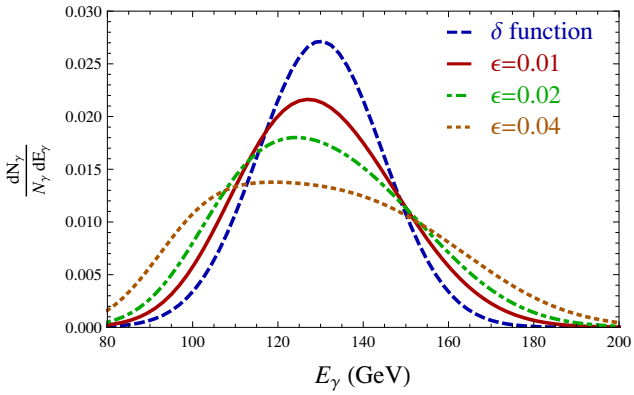

Figure 7. The energy-smeared rectangular photon spectra of eq. (4.3) for different values of the mass splitting ϵ. The dark matter mass is chosen to be 260 GeV for the red solid, green dotdashed, orange dotted lines. As a comparison, we also show a smeared delta function at 130 GeV in the blue dashed line.

which, as $\epsilon \equiv m_\chi/m_\phi - 1 \to 0$, limits to a delta function centered at $m_\chi/2$. Here $\Theta(x)$ is the usual Heavyside function.

Since the gamma line spectrum can provide a good fit to Fermi LAT data, we also anticipate a good fit for this model for sufficiently small ϵ. To estimate upper bounds for ϵ, we consider the average Fermi-LAT energy resolution for gamma ray energies above 50 GeV, $\sigma(E)/E \approx 0.10 + 0.0001\, E/\text{GeV}$ [45]. We use this energy resolution to smear the spectra in eq. (4.3) for different values of ϵ and compare them with a smeared delta function spectrum centered at 130 GeV. The results are shown in figure 7, where we have shown three different values of $\epsilon = 0.01, 0.02, 0.04$ in the red solid, green dot-dashed, and orange dotted lines. The delta function spectrum is shown in the blue dashed line. As one can see, once $\mathcal{O}(\sqrt{\epsilon}/2)$ is smaller than the energy resolution (order 10%) the distinctions between the smeared delta function and the smeared cascade spectra are minimal.

To work out the parameter space for this model we translate the best-fit line spectra of [8] to the cascade model. Since the photon flux from dark matter annihilation is inversely proportional to the square of the DM mass, and there are now four photons in the final state, the required annihilation cross section for this case should be approximately twice that found for a photon line. Thus we require $\langle\sigma v\rangle_0 = 0.168$ pb·c for the Einasto profile and 0.304 pb·c for the NFW profile.

Our explicit model considers fermionic DM and, for economy, a single real scalar ϕ. Thus parity dictates that the annihilation is p-wave suppressed unless both λ_χ^r and the CP-violating λ_χ^i are nonzero. In terms of the mass splitting ϵ, the cross-section for $\overline{\chi}\chi \to \phi\phi$ is

$$\sigma v = \frac{\lambda_\chi^{r\,2}\lambda_\chi^{i\,2}\sqrt{\epsilon}}{\sqrt{2}\pi m_\chi^2} + v^2\left[\frac{\lambda_\chi^{r\,2}\lambda_\chi^{i\,2}}{16\sqrt{2}\pi m_\chi^2\sqrt{\epsilon}} + \frac{\lambda_\chi^{r\,2}(16\lambda_\chi^{r\,2} - 87\lambda_\chi^{i\,2})\sqrt{\epsilon}}{64\sqrt{2}\pi m_\chi^2}\right] + \mathcal{O}(v^4) \qquad (4.4)$$

where we have kept the leading terms in the limit $\epsilon \ll 1$.

In figure 8, we show the contours in the λ_χ^i-λ_χ^r plane which give the required dark matter annihilation cross section for explaining the Fermi-LAT gamma line excess, for

JHEP12(2012)056

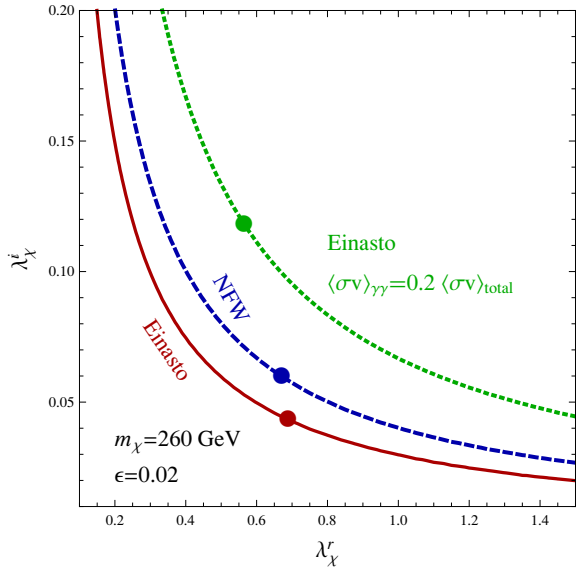

Figure 8. The contours of couplings λ_χ^i and λ_χ^r which yield the best-fit cross-sections for the gamma line excess. The solid circles indicate the points which yield a thermal relic abundance of $\Omega_\chi h^2 = 0.11$. The green dotted line is the case when $\mathrm{Br}(\phi \to \gamma\gamma) = 0.2$ of the total.

$m_\chi = 260\,\mathrm{GeV}$ and $\epsilon = 0.02$. The points which give the relic abundance $\Omega_\chi h^2 = 0.11$ are indicated by heavy circles. Hierarchies of order ~ 10 between CP-preserving and CP-violating couplings are required, suggesting small (but not tiny) CP violation in a DM sector. We also show the case where the branching fraction of ϕ into two photons is 20%.

An equally well-motivated alternative to the CP-violating reference model considered here would be to allow the Dirac DM χ to annihilate to a nearly degenerate pair of scalars with opposite parity, ϕ and a, with subsequent decays to photons. In this case, the s-wave annihilation $\overline{\chi}\chi \to \phi\, a$ is proportional to $(\lambda_\chi^\phi \lambda_\chi^a)^2$, while the p-wave annihilation is proportional to $\sim (\lambda_\chi^\phi)^4 + (\lambda_\chi^a)^4$. If the branching fractions of ϕ, a into photons are order 1, accommodating the dark matter thermal relic abundance and the present-day annihilation cross section for the Fermi-LAT gamma line still requires a factor of ~ 10 hierarchy between λ_χ^ϕ and λ_χ^a.

5 Discussion and conclusions

We have explored the possibilities for thermal models for the Fermi-LAT 130 GeV gamma line excess where the dominant DM annihilation channel is into photons. We consider two mechanisms, (1) models where a resonance in the DM spectrum enhances the annihilation rate during freezeout and to a lesser extent at the present day, and (2) models where DM annihilates to a new intermediate state which subsequently decays to photon pairs. Here the interplay of the s-wave and p-wave annihilation is responsible for reconciling the necessary cross-section at freezeout with the observed cross-section today. For the resonance model, charged fermions at the TeV scale are predicted and are accessible at the Large Hadron Collider [46, 47]. The new charged fermion could be a collider-stable

JHEP12(2012)056

particle. The long-lived charged particle search imposes a lower bound its mass to be above around 250 GeV if its electric charge is one [48]. Introducing additional couplings of the new charged fermion to SM fermions, additional final states at colliders may be studied to fully cover this new charged fermion. For example, the new charged fermion with an electric charge one can behave as a heavy charged lepton and decay into one lepton plus neutrinos. The opposite-sign two leptons plus missing energy searches would be suitable to look for this charged fermion.

Both of the classes of models considered in this paper require coincidences in the mass spectrum. For resonant freezeout, the resonance mass m_a must be within a percent of twice the dark matter mass, a striking coincidence. For cascade decays, the intermediate state(s) ϕ must be within again about a percent of the dark matter mass in order to have a sharp enough spectral feature to fit the data well. These near-degeneracies are suggestive of a dark sector with one scale Λ_m setting the overall mass scale, and another $\Lambda_G \ll \Lambda_m$ determining splittings. Composite dark sectors are an appealing avenue to flesh out the models we have considered. Near-degeneracies in the dark sector spectrum, as necessary for the cascade annihilation model, are readily accommodated in composite sectors. Resonances above threshold pose a somewhat more complicated picture. As we know from heavy quarkonia in the SM, a spectrum with resonances slightly above threshold could certainly be obtained; the complication is that such resonances would necessarily be accompanied by a resonance *below* threshold, giving the thermal relic abundance a detailed dependence on the parameters of the model. We leave detailed model building to future work.

Acknowledgments

We would like to thank Tim Tait, Haibo Yu and especially Simona Murgia for useful discussions and comments. SLAC is operated by Stanford University for the US Department of Energy under contract DE-AC02-76SF00515. JS was supported by the DOE grant DE-FG02-92ER40704 and by the LHC Theory Initiative through the grant NSF-PHY-0969510. We also thank the Aspen Center for Physics, under NSF Grant No. 1066293, where this work was completed.

Open Access. This article is distributed under the terms of the Creative Commons Attribution License which permits any use, distribution and reproduction in any medium, provided the original author(s) and source are credited.

References

[1] L. Bergstrom and H. Snellman, *Observable monochromatic photons from cosmic photino annihilation*, *Phys. Rev.* **D 37** (1988) 3737 [INSPIRE].

[2] Z. Bern, P. Gondolo and M. Perelstein, *Neutralino annihilation into two photons*, *Phys. Lett.* **B 411** (1997) 86 [hep-ph/9706538] [INSPIRE].

[3] L. Bergstrom, T. Bringmann, M. Eriksson and M. Gustafsson, *Two photon annihilation of Kaluza-Klein dark matter*, *JCAP* **04** (2005) 004 [hep-ph/0412001] [INSPIRE].

JHEP12(2012)056

[4] G. Bertone, C. Jackson, G. Shaughnessy, T.M. Tait and A. Vallinotto, *The WIMP forest: indirect detection of a chiral square*, *Phys. Rev.* **D 80** (2009) 023512 [arXiv:0904.1442] [INSPIRE].

[5] G. Bertone, C. Jackson, G. Shaughnessy, T.M. Tait and A. Vallinotto, *γ ray lines from a universal extra dimension*, *JCAP* **03** (2012) 020 [arXiv:1009.5107] [INSPIRE].

[6] LAT collaboration, W. Atwood et al., *The Large Area Telescope on the Fermi γ-ray space telescope mission*, *Astrophys. J.* **697** (2009) 1071 [arXiv:0902.1089] [INSPIRE].

[7] T. Bringmann, X. Huang, A. Ibarra, S. Vogl and C. Weniger, *Fermi LAT search for internal bremsstrahlung signatures from dark matter annihilation*, *JCAP* **07** (2012) 054 [arXiv:1203.1312] [INSPIRE].

[8] C. Weniger, *A tentative γ-ray line from dark matter annihilation at the Fermi Large Area Telescope*, *JCAP* **08** (2012) 007 [arXiv:1204.2797] [INSPIRE].

[9] E. Tempel, A. Hektor and M. Raidal, *Fermi 130 GeV γ-ray excess and dark matter annihilation in sub-haloes and in the galactic centre*, *JCAP* **09** (2012) 032 [*Addendum ibid.* **1211** (2012) A01] [arXiv:1205.1045] [INSPIRE].

[10] M. Su and D.P. Finkbeiner, *Strong evidence for γ-ray line emission from the inner galaxy*, arXiv:1206.1616 [INSPIRE].

[11] A. Hektor, M. Raidal and E. Tempel, *An evidence for indirect detection of dark matter from galaxy clusters in Fermi-LAT data*, arXiv:1207.4466 [INSPIRE].

[12] M. Su and D.P. Finkbeiner, *Double γ-ray lines from unassociated Fermi-LAT sources*, arXiv:1207.7060 [INSPIRE].

[13] D. Hooper and T. Linden, *Are lines from unassociated γ-ray sources evidence for dark matter annihilation?*, *Phys. Rev.* **D 86** (2012) 083532 [arXiv:1208.0828] [INSPIRE].

[14] N. Mirabal, *The dark knight falters*, arXiv:1208.1693 [INSPIRE].

[15] A. Hektor, M. Raidal and E. Tempel, *Double γ-ray lines from unassociated Fermi-LAT sources revisited*, arXiv:1208.1996 [INSPIRE].

[16] R. Cotta et al., *Constraints on the pMSSM from LAT observations of dwarf spheroidal galaxies*, *JCAP* **04** (2012) 016 [arXiv:1111.2604] [INSPIRE].

[17] W. Buchmüller and M. Garny, *Decaying vs. annihilating dark matter in light of a tentative γ-ray line*, *JCAP* **08** (2012) 035 [arXiv:1206.7056] [INSPIRE].

[18] A. Rajaraman, T.M. Tait and D. Whiteson, *Two lines or not two lines? That is the question of γ ray spectra*, *JCAP* **09** (2012) 003 [arXiv:1205.4723] [INSPIRE].

[19] LAT collaboration, M. Ackermann et al., *Fermi LAT search for dark matter in γ-ray lines and the inclusive photon spectrum*, *Phys. Rev.* **D 86** (2012) 022002 [arXiv:1205.2739] [INSPIRE].

[20] A. Boyarsky, D. Malyshev and O. Ruchayskiy, *Spectral and spatial variations of the diffuse γ-ray background in the vicinity of the Galactic plane and possible nature of the feature at 130 GeV*, arXiv:1205.4700 [INSPIRE].

[21] F. Aharonian, D. Khangulyan and D. Malyshev, *Cold ultrarelativistic pulsar winds as potential sources of galactic gamma-ray lines above 100 GeV*, arXiv:1207.0458 [INSPIRE].

[22] T. Cohen, M. Lisanti, T.R. Slatyer and J.G. Wacker, *Illuminating the 130 GeV γ line with continuum photons*, *JHEP* **10** (2012) 134 [arXiv:1207.0800] [INSPIRE].

JHEP12(2012)056

[23] I. Cholis, M. Tavakoli and P. Ullio, *Searching for the continuum spectrum photons correlated to the* 130 *GeV* γ*-ray line*, *Phys. Rev.* **D 86** (2012) 083525 [arXiv:1207.1468] [INSPIRE].

[24] X.-Y. Huang, Q. Yuan, P.-F. Yin, X.-J. Bi and X.-L. Chen, *Constraints on the dark matter annihilation scenario of Fermi* 130 *GeV* γ*-ray line emission by continuous* γ*-rays, Milky Way halo, galaxy clusters and dwarf galaxies observations*, *JCAP* **11** (2012) 048 [arXiv:1208.0267] [INSPIRE].

[25] J.M. Cline, 130 *GeV dark matter and the Fermi* γ*-ray line*, *Phys. Rev.* **D 86** (2012) 015016 [arXiv:1205.2688] [INSPIRE].

[26] D. Das, U. Ellwanger and P. Mitropoulos, *A* 130 *GeV photon line from dark matter annihilation in the NMSSM*, *JCAP* **08** (2012) 003 [arXiv:1206.2639] [INSPIRE].

[27] D. Larson et al., *Seven-year Wilkinson Microwave Anisotropy Probe (WMAP) observations: power spectra and WMAP-derived parameters*, *Astrophys. J. Suppl.* **192** (2011) 16 [arXiv:1001.4635] [INSPIRE].

[28] B.S. Acharya, G. Kane, S. Watson and P. Kumar, *A non-thermal WIMP miracle*, *Phys. Rev.* **D 80** (2009) 083529 [arXiv:0908.2430] [INSPIRE].

[29] S. Tulin, H.-B. Yu and K.M. Zurek, *Three exceptions for thermal dark matter with enhanced annihilation to* $\gamma\gamma$, arXiv:1208.0009 [INSPIRE].

[30] N. Weiner and I. Yavin, *How dark are Majorana WIMPs? Signals from MiDM and Rayleigh dark matter*, *Phys. Rev.* **D 86** (2012) 075021 [arXiv:1206.2910] [INSPIRE].

[31] K. Griest and D. Seckel, *Three exceptions in the calculation of relic abundances*, *Phys. Rev.* **D 43** (1991) 3191 [INSPIRE].

[32] H.M. Lee, M. Park and W.-I. Park, *Fermi* γ *ray line at* 130 *GeV from axion-mediated dark matter*, *Phys. Rev.* **D 86** (2012) 103502 [arXiv:1205.4675] [INSPIRE].

[33] Z. Kang, T. Li, J. Li and Y. Liu, *Brightening the (*130 *GeV)* γ*-ray line*, arXiv:1206.2863 [INSPIRE].

[34] J. Bagnasco, M. Dine and S.D. Thomas, *Detecting technibaryon dark matter*, *Phys. Lett.* **B 320** (1994) 99 [hep-ph/9310290] [INSPIRE].

[35] V. Barger, W.-Y. Keung and D. Marfatia, *Electromagnetic properties of dark matter: dipole moments and charge form factor*, *Phys. Lett.* **B 696** (2011) 74 [arXiv:1007.4345] [INSPIRE].

[36] J.M. Cline, A.R. Frey and G.D. Moore, *Composite magnetic dark matter and the* 130 *GeV line*, arXiv:1208.2685 [INSPIRE].

[37] G. Jungman, M. Kamionkowski and K. Griest, *Supersymmetric dark matter*, *Phys. Rept.* **267** (1996) 195 [hep-ph/9506380] [INSPIRE].

[38] B.A. Kniehl and M. Spira, *Low-energy theorems in Higgs physics*, *Z. Phys.* **C 69** (1995) 77 [hep-ph/9505225] [INSPIRE].

[39] E. Dudas, Y. Mambrini, S. Pokorski and A. Romagnoni, *Extra* U(1) *as natural source of a monochromatic* γ *ray line*, *JHEP* **10** (2012) 123 [arXiv:1205.1520] [INSPIRE].

[40] M. Ibe, H. Murayama and T. Yanagida, *Breit-Wigner enhancement of dark matter annihilation*, *Phys. Rev.* **D 79** (2009) 095009 [arXiv:0812.0072] [INSPIRE].

[41] J. Mardon, Y. Nomura, D. Stolarski and J. Thaler, *Dark matter signals from cascade annihilations*, *JCAP* **05** (2009) 016 [arXiv:0901.2926] [INSPIRE].

JHEP12(2012)056

[42] Y. Bai, M. Carena and J. Lykken, *The PAMELA excess from neutralino annihilation in the NMSSM*, *Phys. Rev.* **D 80** (2009) 055004 [arXiv:0905.2964] [INSPIRE].

[43] J.-F. Fortin, J. Shelton, S. Thomas and Y. Zhao, *γ ray spectra from dark matter annihilation and decay*, arXiv:0908.2258 [INSPIRE].

[44] A. Ibarra, S. Lopez Gehler and M. Pato, *Dark matter constraints from box-shaped γ-ray features*, *JCAP* **07** (2012) 043 [arXiv:1205.0007] [INSPIRE].

[45] FERMI-LAT collaboration, *Fermi LAT performance*, http://www.slac.stanford.edu/exp/glast/groups/canda/lat_Performance.htm.

[46] ATLAS collaboration, *Observation of a new particle in the search for the standard model Higgs boson with the ATLAS detector at the LHC*, *Phys. Lett.* **B 716** (2012) 1 [arXiv:1207.7214] [INSPIRE].

[47] CMS collaboration, *Observation of a new boson at a mass of* 125 *GeV with the CMS experiment at the LHC*, *Phys. Lett.* **B 716** (2012) 30 [arXiv:1207.7235] [INSPIRE].

[48] CMS collaboration, *Search for heavy long-lived charged particles in pp collisions at $\sqrt{s} = 7$ TeV*, *Phys. Lett.* **B 713** (2012) 408 [arXiv:1205.0272] [INSPIRE].

JHEP12(2012)056